Journal of Zhejiang University SCIENCE
ISSN 1009-3095
http://www.zju.edu.cn/jzus
E-mail: jzus@zju.edu.cn

JZUS

Non-axisymmetric instability in the Taylor-Couette flow of fiber suspension*

WAN Zhan-hong (万占鸿)[1], LIN Jian-zhong (林建忠)[†‡1], YOU Zhen-jiang (游振江)[2]

([1]*Department of Mechanics, the State Key Laboratory of Fluid Power Transmission and Control, Zhejiang University, Hangzhou 310027, China*)

([2]*School of Informatics and Engineering, Flinders University of South Australia, GPO Box 2100, Adelaide, SA 5001, Australia*)

[†]E-mail: jzlin@sfp.zju.edu.cn

Received Jan. 20, 2005; revision accepted Mar. 16, 2005

Abstract: An analysis of the instability in the Taylor-Couette flow of fiber suspensions with respect to the non-axisymmetric disturbances was performed. The constitutive model proposed by Ericksen was used to represent the role of fiber additives on the stress tensor. The generalized eigenvalue equation governing the hydrodynamic stability of the system was solved using a direct numerical procedure. The results showed that the fiber additives can suppress the instability of the flow. At the same time, the non-axisymmetric disturbance is the preferred mode that makes the fiber suspensions unstable when the ratio of the angular velocity of the outer cylinder to that of the inner cylinder is a large negative number.

Key words: Fiber suspensions, Taylor-Couette flow, Hydrodynamic instability
doi:10.1631/jzus.2005.AS0001 **Document code:** A **CLC number:** O359

INTRODUCTION

Fiber suspensions have more and more uses in a variety of industrial applications such as the manufacture of composites, environmental, chemical, textile engineering, papermaking, etc. The spatial and orientation distributions of fibers have significant effect on the suspensions (Lin and You, 2003; Lin and Zhang, 2003; Zhou and Lin, 2005). For example, the composite is stiffer and stronger in the direction of greatest orientation, and weaker and more compliant in the direction of least orientation. In researches on fiber suspensions, their hydrodynamic instability is an important topic, so inquiring into the characteristics of their hydrodynamic instability is worthwhile.

Only limited attention, however, have been devoted to the instability of fiber suspensions up to now. Azaiez (2000a; 2000b) presented the results of a linear instability analysis of the mixing layer at high Reynolds numbers, and showed the effects of the presence of rigid fibers on the temporal instability of the flow. You *et al*.(2004) used slender body theories to conduct linear instability analysis of the circular pipe and channel flow in the presence of fiber additives. Pilipenko *et al*.(1981) discussed theoretically the effect of fibers on the instability of the laminar Taylor-Couette flow of fiber suspensions using the model of an anisotropic Ericksen fluid in the case of weak Brownian motion. It was found that the fibers suppressed the instability of the flows at which the realization of a secondary steady periodic flow is possible by resolving the linear instability under the condition of narrow gap approximation. Blaise (1994) carried out an instability analysis of the rigid fiber suspensions using the rheological coefficients in the Ericksen anisotropic fluid state equation that Pilipenko used in the case of wide-gap, and indicated that the fibers enhanced the stability of the flow. Gupta *et al*.(2002) investigated the centrifugal instability of the Taylor-Couette flow in a semi-concentration non-Brownian fiber suspension by utilizing the fiber orien-

[‡]Corresponding author

[*]Project (No. 10372090) supported by the National Natural Science Foundation of China

tation model in conjunction with a quadratic and hybrid closure approximation, with the results showing that the fiber additives can suppress the instability of flow. In general, fiber additives tend to reduce the instability of the flow based on the above results. However, the investigations mentioned above are based on the assumptions that steady secondary flow coexists with axisymmetric disturbances, and that the outer cylinder is stationary while the inner cylinder rotates. Present literatures have not reported investigations on the hydrodynamic instability of fiber suspensions by introducing non-axisymmetric disturbances. Therefore, the aim of this work is to study the effect of the non-axisymmetric disturbances on the hydrodynamic instability of fiber suspensions.

MATHEMATICAL MODEL

The assumed to be incompressible fluid is contained between two concentric rotating cylinders whose inner and outer angular velocities and radii are Ω_1, Ω_2 and R_1, R_2, respectively. For infinitely long cylinders, the relevant parameter characterizing the geometry of the flow is the ratio of the two radii of the cylinders $\eta=R_1/R_2$ and the gap between the two cylinders $\delta=R_1-R_2$. The governing equations are the continuity equation and momentum equation:

$$\nabla\cdot\boldsymbol{u}=0, \tag{1}$$

$$\rho\left(\frac{\partial\boldsymbol{u}}{\partial t}+\boldsymbol{u}\cdot\nabla\boldsymbol{u}\right)=-\nabla p+\nabla\cdot\boldsymbol{\tau}, \tag{2}$$

where ρ, p are the density and the isotropic pressure of the fluid, respectively, $\boldsymbol{u}$ is the velocity vector, $\boldsymbol{u}=u\boldsymbol{e}_r+v\boldsymbol{e}_\theta+w\boldsymbol{e}_z$, $\boldsymbol{\tau}$ is the stress tensor. The boundary condition on the cylinder walls is no-slip condition.

According to the invariant theory of anisotropic fluids (Erickson, 1960), the stress tensor $\boldsymbol{\tau}$ can be expressed as a function dependent on the velocity gradient and the fiber preferred direction:

$$\boldsymbol{\tau}=2\mu\dot{\boldsymbol{\gamma}}+(\mu_1+\mu_2\dot{\boldsymbol{\gamma}}:\boldsymbol{nn})\boldsymbol{nn}+2\mu_3(\dot{\boldsymbol{\gamma}}\cdot\boldsymbol{nn}+\boldsymbol{nn}\cdot\dot{\boldsymbol{\gamma}}) \tag{3}$$

where $\dot{\boldsymbol{\gamma}}$ is the tensor of strain rate and defined as

$$\dot{\boldsymbol{\gamma}}=(\nabla\boldsymbol{u}^{\mathrm{T}}+\nabla\boldsymbol{u})/2, \tag{4}$$

For brevity, we denote:

$$\boldsymbol{\tau}^{f}=(\mu_1+\mu_2\dot{\boldsymbol{\gamma}}:\boldsymbol{nn})\boldsymbol{nn}+2\mu_3(\dot{\boldsymbol{\gamma}}\cdot\boldsymbol{nn}+\boldsymbol{nn}\cdot\dot{\boldsymbol{\gamma}}) \tag{5}$$

$\boldsymbol{n}$ in Eq.(3) represents the preferred direction of the fibers, and the material derivative of $\boldsymbol{n}$ satisfies:

$$\frac{\partial\boldsymbol{n}}{\partial t}+\boldsymbol{u}\cdot\nabla\boldsymbol{n}=\boldsymbol{\omega}\cdot\boldsymbol{n}+\chi(\dot{\boldsymbol{\gamma}}\cdot\boldsymbol{n}-\dot{\boldsymbol{\gamma}}:\boldsymbol{nnn}), \tag{6}$$

where $\boldsymbol{\omega}$ is the vorticity tensor and defined by

$$\boldsymbol{\omega}=(\nabla\boldsymbol{u}^{\mathrm{T}}-\nabla\boldsymbol{u})/2, \tag{7}$$

χ in Eq.(6) is a geometric parameter related to the fiber aspect ratio $H=L/d$ with L and d being the length and the diameter of the fiber. Hand (1961) compared the above equations with Jeffery's equation for ellipsoid and found that both equations are identical with an appropriate interpretation of the material constant $\chi=(H^2-1)/(H^2+1)$, with χ is equal to zero for a spherical particle, while for the fibers, χ acts as a shape factor and approaches unity when the fiber aspect ratio approaches infinity. In Eq.(3), μ_1, μ_2 and μ_3 are the independent material constants. It can be found that the fluid with non-zero μ_1 is the Bingham fluid if the fluid is at rest. In the present study μ_1 is zero. μ_2 and μ_3 are derived based on different theories. When Brownian motion is absent or weak, μ_2 and μ_3 depend mainly on the fiber properties such as the aspect ratio H and the volume concentration ϕ of the fibers. The fourth term on the right hand side of Eq.(3) is significant for fibers that are close to the molecular scale, but can be negligible for relatively large particles. In the semi-concentration regime, i.e. $1/H^2\leq\phi\leq1/H$, several models have been developed to determine the expression of the parameter μ_2. For slender rigid ellipsoids of revolution, Hinch and Leal (1972) and Batchelor (1971) derived the following expressions for μ_2 with aligned fibers subjected to elongation along the fiber axis, respectively:

$$\mu_2=\mu\phi H^2/[\ln(2H)-1.5], \tag{8}$$

$$\mu_2=2\mu\phi H^2/[3\ln(2\pi/\phi)^{1/2}], \tag{9}$$

Pilipenko *et al.*(1981) got a constant parameter μ_2 for large H with the Brownian motion neglected:

$$\mu_2=\mu\phi\{H^2/[\ln(2H)-1.5]-(1.26H/\ln H)\}, \quad (10)$$

Dinh and Armstrong (1984) made essentially equivalent extensions of Bachelor's approach to arbitrary flows based on the slender-body theory. They used cell model to derive the expression of μ_2. Comparing their model with Eq.(3), μ_2 reads:

$$\mu_2=2\mu\phi H^2/[3\ln(2h_f/d)], \quad (11)$$

here h_f is a characteristic distance between a fiber and its nearest neighbors, which depends on the fibers orientation. $h_f/d=(\pi/4\phi)^{1/2}$ for aligned fibers, and $h_f/d=\pi/4\phi H$ for fibers with random orientations.

The contribution of the fibers to the stress is not proportional to their volume concentration according to Eqs.(8) and (10). Shaqfeh and Frederickson (1990) derived the expression of μ_2 based on the thin slender body theory, taking the fiber-fiber interactions into account:

$$\mu_2=4\mu\phi H^2/\{3[\ln(1/\phi)+\ln(\ln(1/\phi))+C]\}, \quad (12)$$

where C is a constant dependent on the distribution of orientation and shape of the fiber. If the fibers are aligned, C=0.1585, whereas C=–0.6634 for an isotropic suspension. It should be pointed out that all these expressions for μ_2 are essentially the same in the range of validity of the theory although they have some differences in the forms. Eq.(12) is adopted here.

To undimensionalize the parameter in the flow, we rescale the dimension by the gap width δ, the time t by the momentum diffusion time δ^2/ν across the gap, the velocity $\boldsymbol{u}$ by Ω_1R_1 of the inner cylinder, and the pressure p by $\rho\Omega_1R_1\nu/\delta$. So the governing Eqs.(1), (2) and (6) can be rewritten in a non-dimensional form:

$$\nabla\cdot\boldsymbol{u}=0, \quad (13)$$

$$\partial\boldsymbol{u}/\partial t+Re(\boldsymbol{u}\cdot\nabla)\boldsymbol{u}=-\nabla p+\nabla\cdot\boldsymbol{\tau}, \quad (14)$$

$$Re^{-1}\partial\boldsymbol{n}/\partial t+\boldsymbol{u}\cdot\nabla\boldsymbol{n}=\boldsymbol{\omega}\cdot\boldsymbol{n}+\chi(\dot{\boldsymbol{\gamma}}\cdot\boldsymbol{n}-\dot{\boldsymbol{\gamma}}:\boldsymbol{nnn}), \quad (15)$$

where the Reynolds numbers of the Couette flow $Re=\Omega_1R_1\delta/\nu$. The boundary conditions are:

At the wall of inner cylinder:

$$r=\eta/(1-\eta),\ u=0,\ v=1,\ w=0, \quad (16)$$

At the wall of outer cylinder:

$$r=1/(1-\eta),\ u=0,\ v=\Omega/\eta,\ w=0, \quad (17)$$

Solution of Eqs.(13) and (14) yields a stationary laminar circular Couette flow:

$$\boldsymbol{u}_0(r)=V_0(r)\boldsymbol{e}_\theta=(Ar+B/r)\boldsymbol{e}_\theta, \quad (18)$$

$$p_0(r)=Re\int_{r_i}^{r}\frac{V_0^2(r)}{r}\mathrm{d}r-N_1N_2(\mu_2+4\mu_3)\frac{B}{r^2} \quad (19)$$

where $A=\dfrac{\Omega-\eta^2}{\eta(1+\eta)}$, $B=\dfrac{\eta(1-\Omega)}{(1-\eta)(1-\eta^2)}$, $\Omega=\Omega_2/\Omega_1$, $N_1=[(1-\chi)/(2\chi)]^{1/2}$, $N_2=[(\chi+1)/(2\chi)]^{1/2}$, $N_3=0$.

Infinitesimally small disturbances are introduced to the basic flow field in the azimuthal θ and axial z directions. Then the velocity, pressure and orientation vectors are expressed by the base flow and the small perturbations.

$$\boldsymbol{u}=(u^*,V_0(r)+v^*,w^*),\ p=p_0(r)+p^*,$$
$$\boldsymbol{n}=(N_1+n_1^*,N_2+n_2^*,N_3+n_3^*).$$

where "*" denote small disturbances. Normal mode analysis revealed that the perturbation parts of the velocity and the pressure can be expressed as:

$$\begin{pmatrix}u^*\\v^*\\w^*\\p^*\end{pmatrix}=\begin{pmatrix}u(r)\\v(r)\\w(r)\\p(r)\end{pmatrix}\exp[\lambda t+\mathrm{i}(m\theta+kz)], \quad (20)$$

and that the orientation vector $\boldsymbol{n}^*$ is:

$$\begin{pmatrix}n_1^*\\n_2^*\\n_3^*\end{pmatrix}=\begin{pmatrix}n_1(r)\\n_2(r)\\n_3(r)\end{pmatrix}\exp[\lambda t+\mathrm{i}(m\theta+kz)], \quad (21)$$

where k, m are the wave numbers in axial and azimuthal direction, respectively, the eigenvalue $\lambda=\lambda_r+\mathrm{i}\lambda_i$ is the growth rate of the perturbation.

By introducing the perturbations Eqs.(20) and (21) into the momentum equations, we can obtain the linear stability equations of fiber suspensions in cylindrical coordinates with consideration of weak Brownian motion. The equations make up a complex generalized eigenvalues problem that can be written in the implicit functional form:

$$F(Re, \Omega, H, \phi, \eta, m, k, \lambda)=0, \quad (22)$$

For a set values of Ω, H, ϕ, η, m and k, we can determine the real positive value of Re when the real value of λ_r is equal to zero. The Chebyshev spectral method, similar to that of by Orszag (1971), is used to solve the above equations numerically. The concept of a differentiation matrix used by Weideman and Reddy (2000) and Trefethen (2000) proved to be a very useful tool for numerically solving differential equations, and is used in the present study to put the Chebyshev spectral method into practice.

RESULTS AND DISCUSSION

In order to assure the validity of the computational procedure, the present results for an axisymmetric Newtonian fluid are compared with other results (Recktenwald *et al.*, 1993). The critical inner Reynolds number Re_c and the critical wave number k_c are listed in Table 1, where η is the ratio of the radius of inner cylinder to that of outer cylinder, when the outer cylinder is stationary. From the table, we can see that both results are in agreement.

Table 1 Comparison of computational results

η	Re_c		k_c	
	Other result	Present result	Other result	Present result
0.8	94.73	94.73	3.1326	3.1328
0.9	131.61	131.61	3.1288	3.1288
0.975	260.95	260.94	3.1270	3.1270

Figs.1 and 2, in which η=0.9, H=10^3, ϕ=10^{-3}, show the effect of fiber additives on the instability of the Taylor-Couette flow. Fig.1 shows the neutral stability curves for three different ratios of the angular velocity of outer cylinder to that of inner cylinder Ω=0.5, 0, –0.5 and for three azimuthal wave numbers m=0, 1, 2, respectively. The Reynolds number in the figure is normalized according to the critical Reynolds numbers for the Newtonian Taylor-Couette flow. It can be seen that the addition of the fibers enhances the critical Reynolds numbers, i.e., the fiber suspensions are more stable than those in the corresponding Newtonian flow. The smaller the axial wave number is, the stronger is the fibers suppression of the flow instability. We can also find that the critical Reynolds numbers is larger when non-axisymmetric disturbances are introduced than that when axisymmetric disturbances are introduced, for Ω=0.5, 0 and –0.5, which means that the axisymmetric disturbances easily make the flow unstable. However, the curves in cases axisymmetric disturbances and of non-axisymmetric disturbances change a lot with increasing Ω.

Fig.2a shows that when Ω=–0.7, the difference of the two curves in the case of axisymmetric disturbances with m=0 and the case of non-axisymmetric

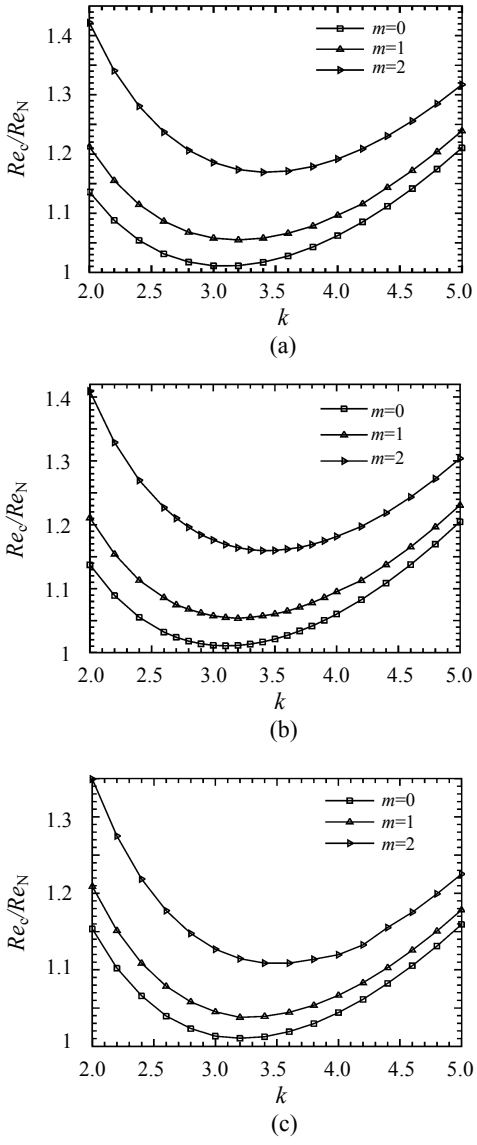

Fig.1 Relative neutral stability curves Re_c/Re_N vs k
(a) Ω=0.5; (b) Ω=0; (c) Ω=–0.5

disturbances with m=1 is small. While as shown in Fig.2b, the critical Reynolds numbers is smaller for the non-axisymmetric disturbances than that for the axicymmetric disturbances when Ω=–1.

Corresponding to Fig.2, Fig.3 shows the variations of the growth rate of the disturbances λ_r versus the axial wave number k for different azmuthal wave number m with a given Reynolds number Re=192 and 245, respectively. We can see that when axisymmetric perturbations dominate in the flow, there is little change of the most unstable axial wave number. But when non-axisymmetric disturbances surpass the axisymmetric ones, the characteristics of instability have some differences. The larger the wave number corresponding to the greatest growth rate of the disturbance in the azimuthal direction is, the smaller is the most unstable axial wave number.

Fig.4 shows the influence of the aspect ratio H on the critical Reynolds numbers Re_c for the axisymmetric disturbance m=0 and non-axisymmetric disturbance $m\neq0$ at η=0.88 and $\phi=10^{-4}$. We can obtain the smallest critical value of inner cylinder Reynolds number for different azimuthal wave numbers by interpolating and drawing the graphs between Re_c and Ω. For a given Ω in Fig.4, the critical Reynolds number Re_c is determined according to the lowest point on the

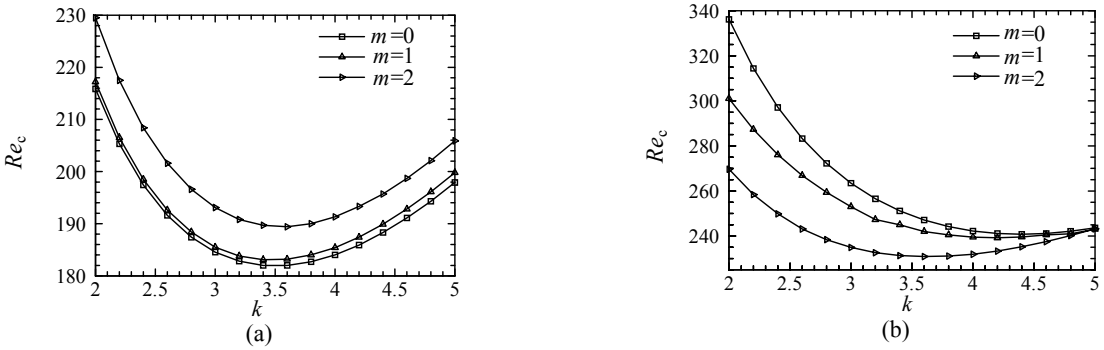

Fig.2 Neutral stability curves Re_c vs k. (a) Ω=–0.7; (b) Ω=–1

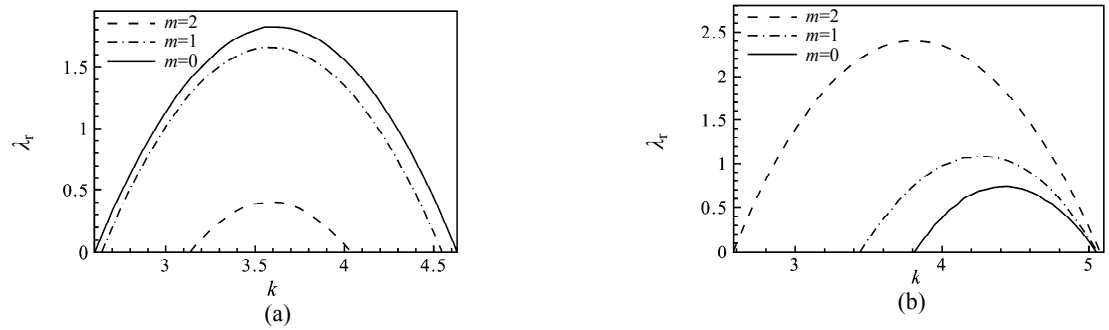

Fig.3 Growth rate of disturbances λ_r vs k. (a) Ω=–0.7; (b) Ω=–1

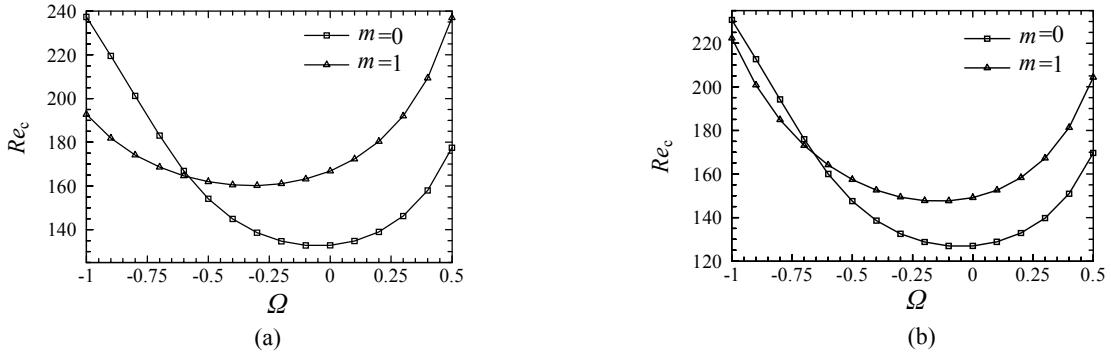

Fig.4 Variation of Re_c vs Ω for different aspect ratio H. (a) $H=10^4$; (b) $H=0.7\times10^4$

neutral stability curves. Comparing Fig.4a with Fig.4b, we can see that the larger Ω is, the more stable is the flow in case of axisymmetric or non-axisymmetric perturbations. At the same time, Ω is equal to –0.58 when H=10^4, i.e., the non-axisymmetric disturbances destabilized the flow more easily than the axisymmetric disturbance when Ω<–0.58. The critical value of Ω is –0.66 for the case of H=0.7×10^4.

The effects of ϕ on the stability can be seen from Fig.5 in which η=0.92 and H=10^4. It can be seen that the effects of the volume concentration of the fibers on the stability are similar to the effects of the fiber aspect ratio. The critical value of Ω is –0.71 for ϕ=0.5×10^{-4}, while Ω is –0.62 for ϕ=10^{-4}, i.e. the critical value of Ω decreases with decreasing volume concentration ϕ.

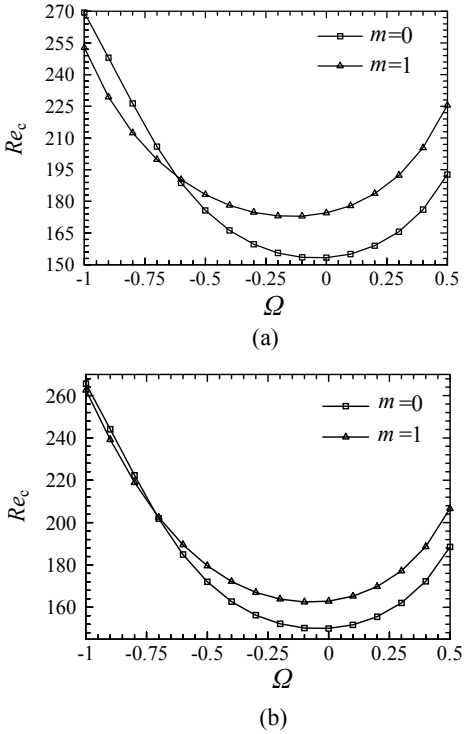

Fig.5 Variation of Re_c vs Ω for different volume fraction ϕ
(a) ϕ=10^{-4}; (b) ϕ=0.5×10^{-4}

It is known that the method of energy balance provides a very useful tool for studying the driving forces of the disturbance and can shed some light on the critical transition. In order to explain the mechanisms of the fiber additives suppression of the instability, we examine the disturbance kinetic energy equation derived by taking the scalar product of the linearized momentum equation with the product of the disturbance velocity vector and radial direction vector, then integrating the resulting equation from R_1 to R_2 (Frigaard and Nouar, 2003). It yields:

$$\lambda\|\boldsymbol{u}\|^2=ReE_{\mathrm{in}}-E_{\mathrm{vi}}-E_{\mathrm{f}}, \tag{23}$$

where

$$\|\boldsymbol{u}\|^2=\int_{R_1}^{R_2} r|\boldsymbol{u}|^2\mathrm{d}r$$

$$E_{\mathrm{in}}=\int_{R_1}^{R_2}\left[2V_0vu^+-(rDV_0+V_0)v^+u-\mathrm{i}mV_0|u|^2\right]\mathrm{d}r$$

$$E_{\mathrm{vi}}=\int_{R_1}^{R_2}\left[r|D\boldsymbol{u}|^2+\left(k^2r+\frac{m^2}{r}\right)|\boldsymbol{u}|^2+\mathrm{i}mv^+p+\frac{|u|^2+|v|^2}{r}-\frac{2\mathrm{i}m}{r}(uv^+-u^+v)\right]\mathrm{d}r$$

$$\begin{aligned}E_{\mathrm{f}}=-\int_{R_1}^{R_2}(&ru^+D\tau_{rr}^f+u^+\tau_{rr}^f-u^+\tau_{\theta\theta}^f+w^+\tau_{rz}^f\\&+\mathrm{i}mu^+\tau_{r\theta}^f+\mathrm{i}mv^+\tau_{\theta\theta}^f+\mathrm{i}mw^+\tau_{\theta z}^f\\&+\mathrm{i}krw^+\tau_{zz}^f+rv^+D\tau_{r\theta}^f+2v^+\tau_{r\theta}^f\\&+rw^+D\tau_{rz}^f+\mathrm{i}kru^+\tau_{rz}^f+\mathrm{i}krv^+\tau_{\theta z}^f)\mathrm{d}r\end{aligned} \tag{24}$$

where "$^+$" stands for the complex conjugate transpose of the small disturbance. The term on the left side in Eq.(23) represents the change rate of the disturbance energy, which is proportional to the growth rate of the disturbance λ. This term becomes very small when the real part of λ is close to zero. The first term E_{in} on the right side of Eq.(23) is the inertial term, corresponding to the rate of production of kinetic energy associated with the convection of the base flow. The other two terms E_{vi} and E_{f} are the viscous diffusion due to the suspending fluid and the fiber-induced diffusion, respectively. Our calculations showed that the inertial term E_{in} remains a positive value and acts as a source term in the equation. The other two terms E_{vi} and E_{f} are dissipative. The term E_{vi} dominates the energy dissipation, which is different from the mixing layer of fiber suspensions where the dissipative term caused by the viscous forces is always negligible. The influence of the volume fraction ϕ on E_{f} for axisymmetric and non-axisymmetric disturbance modes is shown in Fig.6 while η=0.9, H=10^3 and Ω=–1, in which E_{f} is normalized by the source term E_{in} of kinetic energy. It can be seen that E_{f} increases monotonously with increasing volume fraction ϕ. But the magnitude of E_{f} is different for the axisymmetric and

non-axisymmetric disturbance modes at a given ϕ. The value of E_f for the axisymmetric disturbance mode is always smaller than that of the non-axisymmetric disturbance mode. Similar conclusion on the function of the fiber aspect ratio H can be drawn. The positive energy caused by the fiber stress consumes the gross energy of the fluid system and leads to suppression of the flow instability.

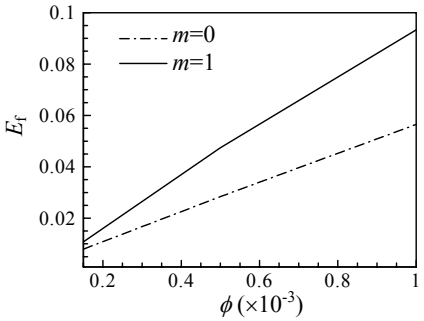

Fig.6 Fiber stress energy E_f vs ϕ

CONCLUSION

The present paper is focused on the effects of fiber additives and the non-axisymmetric disturbances on the hydrodynamic stability of the flow confined between an inner cylinder and a concentric outer cylinder. The numerical results showed that the fibers can suppress the instability of the flow. Furthermore, the suppression is more prominent with increasing volume concentration and aspect ratio of the fiber. For the case, investigated by Gupta *et al*.(2002), of inner cylinder rotating and outer stationary with the axisymmetric modes, the present numerical computations yielded similar results. However, when the ratio of the angular velocity of the outer cylinder to that of the inner cylinder is a large negative number, the assumption that the critical Reynolds number is dependent on the axisymmetric disturbance will not hold in the fiber suspensions, i.e. the instability may be caused firstly by the non-axisymmetric disturbances rather than the axisymmetric disturbances.

References

Azaiez, J., 2000a. Linear stability of free shear flows of fiber suspensions. *J. Fluid Mech.*, **404**:179-209.

Azaiez, J., 2000b. Reduction of free shear flows instability: Effects of polymer versus fiber additives. *J. Non-Newtonian Fluid Mech.*, **91**:233-254.

Batchelor, G.K., 1971. The stress generated in a non-dilute suspension of elongational particles by pure straining. *J. Fluid Mech.*, **46**:813-829.

Blaise, N., 1994. Transition from circular Couette flow to Taylor vortex flow in dilute and semi-concentrated suspensions of stiff fibers. *J. Phys. II France*, **4**:9-22.

Dinh, S.M., Armstrong, R.C., 1984. A rheological equation state for semi-concentrated fiber suspensions. *J. Rheol*., **28**:207-227.

Erickson, J.L., 1960. Transversely isotropic fluids. *Kolloid Z*., **173**:117-122.

Gupta, V.K., Sureshkumar, R., Khomami, B., Azaiez, J., 2002. Centrifugal instability of semidilute non-Brownian fiber suspensions. *J. Phys. Fluids*, **14**:1958-1971.

Hand, G.L., 1961. A theory of dilute suspensions. *Arch. Rat. Mech. Anal*., **7**:81-86.

Hinch, E.J., Leal, L.G., 1972. The effect of Brownian motion on the rheological properties of a suspension of non-spherical particles. *J. Fluid Mech.*, **52**:683-712.

Frigaard, I., Nouar, C., 2003. On three-dimensional linear stability of Poiseuille flow of Bingham fluids. *Phys. Fluids*, **15**:2843-2851.

Lin, J.Z., You, Z.J., 2003. Stability in the circular pipe flow of fiber suspensions. *Journal of Hydrodynamics*, **2**:12-18.

Lin, J.Z., Zhang, L.X., 2003. On the structural features of fiber suspensions in converging channel flow. *Journal of Zhejiang University SCIENCE*, **4**(4):400-406.

Orszag, S.A., 1971. An accurate solution of the Orr-Sommerfeld equation. *J Fluid Mech*., **50**:689-703.

Pilipenko, V.N., Kalinichenko, N.M., Lemak, A.S., 1981. Stability of the flow of a fiber suspension in the gap between coaxial cylinders. *Sov. Phys. Dokl*., **26**: 646-648.

Recktenwald, A., Lucke, M., Muller, H.W., 1993. Taylor vortex formation in axial through-flow: Linear and weakly nonlinear analysis. *Phys. Rev. E*, **48**(6):4444-4454.

Shaqfeh, E.S.G., Frederickson, G.H., 1990. The hydrodynamic stress in a suspension of rods. *Phys. Fluids*, **2**:7-24.

Trefethen, L.N., 2000. Spectral Methods in MATLAB. SIAM, Philadelphia, PA.

Weideman, J.A.C., Reddy, S.C., 2000. A MATLAB differentiation matrix suite. *ACM Transaction on Mathematical Software*, **26**(4):465-519.

You, Z.J., Lin, J.Z., Yu, Z.S., 2004. Hydrodynamic instability of fibre suspensions in channel flows. *Fluid Dynamics Research*, **34**(4):251-271.

Zhou, K., Lin, J.Z., 2005. Research on the behavior of fiber orientation probability distribution function in the planar flows. *Journal of Zhejiang University SCIENCE*, **6A**(4):257-264.